RSC Advances

PAPER

View Article Online
View Journal | View Issue

Cite this: *RSC Adv.*, 2015, **5**, 4261

Simplified phosphorescent organic light-emitting devices using heavy doping with an Ir complex as an emitter

Yanqin Miao,[ab] Xiaogang Du,[ab] Hua Wang,*[ab] Huihui Liu,[ab] Husheng Jia,[ac] Bingshe Xu,[ab] Yuying Hao,[a] Xuguang Liu,[ad] Wenlian Li[e] and Wei Huang[fg]

Received 28th October 2014
Accepted 3rd December 2014

DOI: 10.1039/c4ra13308k

www.rsc.org/advances

Simplified phosphorescent light-emitting devices with the structure ITO/MoO_3 (3 nm)/4,4′-bis(9*H*-carbazol-9-yl)biphenyl (CBP): *x* wt% tris(2-phenylpyridine)iridium(III) [Ir(ppy)$_3$] (30 nm)/3-(biphenyl-4-yl)-4-phenyl-5-(4-*tert*-butylphenyl)-4*H*-1,2,4-triazole (50 nm)/LiF (1 nm)/Al (100 nm) are demonstrated. The optimized organic light-emitting diode with CBP: 25 wt% Ir(ppy)$_3$ as a light-emitting layer showed a peak current efficiency of 46.8 cd A^{-1}, which is 1.64 times that of the reference device with the structure ITO/*N*,*N*′′-bis(naphthalen-1-yl)-*N*,*N*′-bis(phenyl)benzidine (30 nm)/CBP: 8 wt% Ir(ppy)$_3$ (30 nm)/2,9-dimethyl-4,7-diphenyl-1,10-phenanthroline (10 nm)/(4,7-diphenyl-1,10-phenanthroline) (40 nm)/LiF (1 nm)/Al (100 nm). The improvement in efficiency is attributed to the charge-trapping effect of the heavy doping of Ir(ppy)$_3$ and the excellent hole-transporting ability of the CBP layer doped with Ir(ppy)$_3$. When we incorporated bis(4,6-difluorophenyl-pyridine)(picolinate)iridium(III) into the CBP: 25 wt% Ir(ppy)$_3$ layer, the device showed a higher efficiency of 71.2 cd A^{-1}, which is superior to that of previously reported simplified organic light-emitting diodes.

1. Introduction

Phosphorescent organic light-emitting diodes (PhOLEDs) are attracting increasing attention because they can harvest both triplet and singlet excitons, leading to a maximum internal quantum efficiency of 100%.[1–4] *fac*-Tris(2-phenylpyridine) iridium [Ir(ppy)$_3$] is a green phosphor emitter that has been widely used in organic light-emitting diodes (OLEDs). In general, PhOLEDs with a high electroluminescence (EL) efficiency originate from the combination of high-performance phosphor dopants and state-of-the-art device structures. Considerable efforts have been made in recent years to increase the EL performance of Ir(ppy)$_3$ by improving the device structure, such as the insertion of additional organic layers as excitons and charge carrier blockers. Although these insertions generally lower the energy barriers for efficient hole injection and transportation to the emission zone,[5–7] they also result in an increased number of interfaces and complicated device fabrication processes as a result of the increase in the number of functional organic layers. There has therefore been a number of attempts to simplify these OLED structures.[8–11] Simplification based on the direct charge recombination mechanism of Ir(ppy)$_3$ is a practicable solution in terms of fabrication. A significantly simplified OLED structure can be obtained by using heavy doping with Ir(ppy)$_3$. Ir(ppy)$_3$ shows remarkable charge-trap effects and electron-withdrawing ability induced by its 2-phenylpyridine (ppy) ligand.[12,13] Therefore, in a host doped with Ir(ppy)$_3$, electrons are transferred from the HOMO level of the host to that of the Ir(ppy)$_3$ emitter, resulting in the formation of free holes.[14]

We designed a simplified OLED structure in which 4,4′-bis(9*H*-carbazol-9-yl)biphenyl (CBP) doped with Ir(ppy)$_3$ [CBP:Ir(ppy)$_3$] serves both as a hole-transporting layer (HTL) and a light-emitting layer (LEL). The simplified OLED had a higher efficiency than the reference device. The EL mechanism of the simplified OLED is discussed in detail and the improvement in efficiency is attributed to the charge-trapping effect of Ir(ppy)$_3$ and the excellent hole-transporting ability of

[a]*Key Laboratory of Interface Science and Engineering in Advanced Materials, Taiyuan University of Technology, Ministry of Education, No. 79 Yingze Street, Taiyuan 030024, Shanxi, China. E-mail: wanghua001@tyut.edu.cn; Fax: +86-351-6010311; Tel: +86-351-6014852*

[b]*Research Center of Advanced Materials Science and Technology, Taiyuan University of Technology, Taiyuan 030024, China*

[c]*College of Materials Science and Engineering, Taiyuan University of Technology, Taiyuan, 030024, China*

[d]*College of Chemistry and Chemical Engineering, Taiyuan University of Technology, Taiyuan, 030024, China*

[e]*State Key Laboratory of Luminescence and Applications, Changchun Institute of Optics, Fine Mechanics and Physics, Chinese Academy of Sciences, 3888-Dongnanhu Road, Changchun, 130033, China*

[f]*Key Laboratory for Organic Electronics & Information Displays (KLOEID) and Institute of Advanced Materials, Nanjing University of Posts and Telecommunications, Nanjing 210046, China*

[g]*Jiangsu-Singapore Joint Research Center for Organic/Bio-Electronics & Information Displays and Institute of Advanced Materials (IAM), Nanjing Tech University, Nanjing 211816, China*

CBP:Ir(ppy)$_3$. When we incorporated bis(4,6-difluorophenylpyridine)(picolinate)iridium(III) (FIrpic) into the CBP: 25 wt% Ir(ppy)$_3$ layer, the device had an efficiency of 71.2 cd A^{-1}, which is superior to that of previously reported simplified OLEDs.

2. Experimental

All devices were fabricated by vacuum deposition on a pre-patterned indium tin oxide (ITO) glass substrate with a sheet resistance of 15 Ω sq^{-1}. The ITO substrates used as the anode were scrubbed and sonicated consecutively with detergent water, deionized water, and acetone. They were then dried in a drying cabinet and exposed to a UV–ozone environment for 10 min. The substrates were then transferred into a vacuum chamber for the sequential deposition of the organic functional layers by thermal evaporation under a vacuum of 5 × 10^{-4} Pa. The deposition rates for the organic materials, molybdenum trioxide (MoO_3), lithium fluoride (LiF) and Al were about 1, 0.3, 0.1 and 3 Å s^{-1}, respectively. The thickness and deposition rates of the films were controlled by a quartz thickness monitor. The overlap between the ITO anode and the Al cathode was 3 mm × 3 mm and formed the active emissive area of the devices. The performance of the devices was characterized with a PR655 Spectrascan spectrometer and a Keithley 2400 programmable voltage current source. All the samples were measured directly after fabrication (without encapsulation) in an ambient atmosphere at room temperature in a darkroom.

Series A devices were fabricated with different concentrations of dopant and reference devices. The structure of the series A devices was: ITO/MoO_3 (3 nm)/CBP: *x* wt% Ir(ppy)$_3$ (30 nm)/3-(biphenyl-4-yl)-4-phenyl-5-(4-*tert*-butylphenyl)-4*H*-1,2,4-triazole (TAZ) (50 nm)/LiF (1 nm)/Al (100 nm), where *x* is 8, 15, 20, 25 and 30, respectively. The reference device (device R) had the structure: ITO/*N*,*N*′-bis(naphthalen-1-yl)-*N*,*N*′-bis(phenyl) benzidine (NPB) (30 nm)/CBP: 8 wt% Ir(ppy)$_3$ (30 nm)/2,9-dimethyl-4,7-diphenyl-1,10-phenanthroline (BCP) (10 nm)/(4,7-diphenyl-1,10-phenanthroline) (Bphen) (40 nm)/LiF (1 nm)/Al (100 nm).[15] Table 1 summarizes the EL performance of the series A devices and the reference device.

3. Results and discussion

Fig. 1 shows the current efficiency–current density characteristics of the series A devices and device R. The inset in Fig. 1 is a schematic energy level diagram of the series A devices. Fig. 2 shows the current density–voltage–luminance characteristics of the series A devices. From Fig. 1 and Table 1, it can be seen that as the doping concentration of Ir(ppy)$_3$ increased from 8 to 25 wt%, the current efficiency of the series A devices showed a remarkable improvement. When the concentration of Ir(ppy)$_3$ reached 25%, device A4 exhibited a maximum current efficiency of 46.8 cd A^{-1} at a luminance of 60 cd m^{-2}, which is 1.64 times that of device R. At Ir(ppy)$_3$ concentrations >25%, the current efficiency decreased as the doping concentration of Ir(ppy)$_3$ increased. Fig. 2 and Table 1 show that, as the doping concentration of Ir(ppy)$_3$ increased from 8 to 25 wt%, the turn-on

Table 1 Optoelectric characteristics of various PhOLED devices

Device	Device structure	Turn-on voltage[a] (V)	Max. luminance (cd m^{-2})	Max. current efficiency (cd A^{-1})	Current efficiency[b] (cd A^{-1})
R	NPB (30 nm)/CBP: 8 wt% Ir(ppy)$_3$ (30 nm)/BCP (10 nm)/Bphen (40 nm)	3.0	41 448	28.6	28.1
A1	MoO_3 (3 nm)/CBP: 8 wt% Ir(ppy)$_3$ (30 nm)/TAZ (50 nm)	3.0	18 797	32.0	31.6
A2	MoO_3 (3 nm)/CBP: 15 wt% Ir(ppy)$_3$ (30 nm)/TAZ (50 nm)	2.7	20 562	35.1	33.2
A3	MoO_3 (3 nm)/CBP: 20 wt% Ir(ppy)$_3$ (30 nm)/TAZ (50 nm)	2.4	26 952	39.9	38.0
A4	MoO_3 (3 nm)/CBP: 25 wt% Ir(ppy)$_3$ (30 nm)/TAZ (50 nm)	2.4	30 114	46.8	40.7
B1	MoO_3 (1 nm)/CBP: 20 wt% Ir(ppy)$_3$ (30 nm)/TAZ (50 nm)	2.4	18 133	36.7	34.9
B2	MoO_3 (3 nm) CBP: 20 wt% Ir(ppy)$_3$ (30 nm)/TAZ (50 nm)	2.4	26 067	39.2	35.4
B3	MoO_3 (6 nm)/CBP: 20 wt% Ir(ppy)$_3$ (30 nm)/TAZ (50 nm)	2.7	13 292	35.6	34.0
B4	MoO_3 (8 nm)/CBP: 20 wt% Ir(ppy)$_3$ (30 nm)/TAZ (50 nm)	2.7	9002	28.6	27.0
C1	MoO_3 (3 nm)/CBP: 20 wt% Ir(ppy)$_3$: 0 wt% FIrpic (30 nm)/TAZ (50 nm)	2.7	25 150	39.5	34.0
C2	MoO_3 (3 nm)/CBP: 20 wt% Ir(ppy)$_3$: 4 wt% FIrpic (30 nm)/TAZ (50 nm)	2.4	27 524	71.2	67.9
C3	MoO_3 (3 nm)/CBP: 20 wt% Ir(ppy)$_3$: 8 wt% FIrpic (30 nm)/TAZ (50 nm)	2.4	25 905	66.9	62.5

[a] Measured at a luminance of 1 cd m^{-2}. [b] Measured at a luminance of 100 cd m^{-2}.

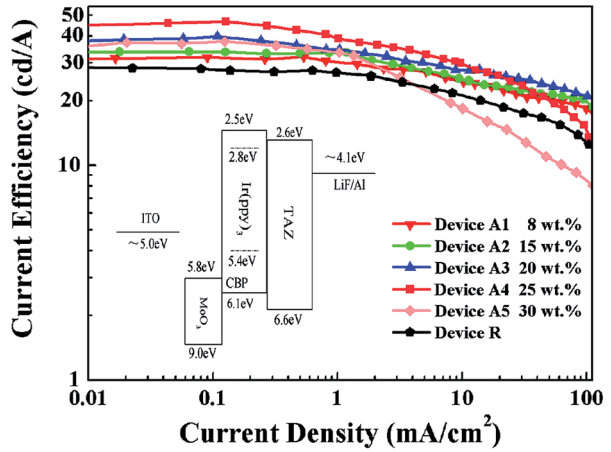

Fig. 1 Current efficiency–current density characteristics of series A devices and device R. Inset: schematic energy level diagram of the series A devices.

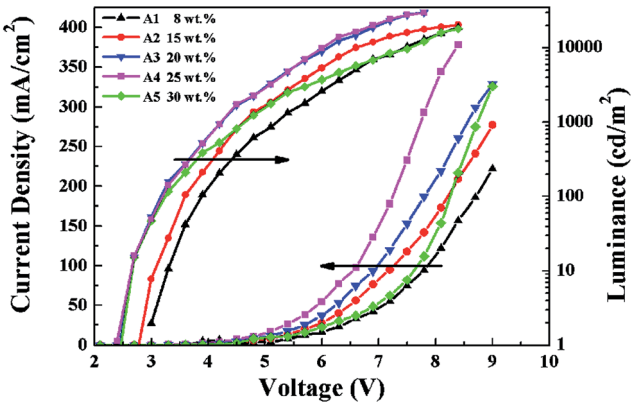

Fig. 2 Current density–voltage–luminance characteristics of the series A devices.

voltage of the series A devices also decreased and device A3 and device A4 had the lowest turn-on voltage of 2.4 V.

When the doping concentration of phosphor exceeds 8 wt%, the EL intensity of PhOLEDs usually decreases at higher current densities as a result of triplet–triplet annihilation and triplet–polaron quenching.[16,17] It was surprising that this phenomenon did not occur in the series A devices. This may be closely related to the direct charge-trapping effect of $Ir(ppy)_3$ in CBP, *i.e.* the majority of the electrons/holes should be trapped by $Ir(ppy)_3$ molecules because the LUMO and HOMO levels of $Ir(ppy)_3$ are located between those of CBP, leading to a direct charge recombination on the $Ir(ppy)_3$ trapping center with a slight energy loss. The charge-trapping effect can further extend all of the hole–electron CBP:$Ir(ppy)_3$ layer from the recombination interface of the LEL/electron-transporting layer (ETL), which can relieve the quenching of emitter excitons as a result of a decrease in the exciton density.[18] The optimum doping concentration of $Ir(ppy)_3$ in CBP is therefore 25 wt%.

3.1. Hole-transporting properties

To validate whether the charge-transporting performance of the CBP: *x* wt% $Ir(ppy)_3$ layer is dependent on the doping concentration of $Ir(ppy)_3$, a series of hole-only devices with the structure ITO/MoO_3 (3 nm)/CBP: *x* wt% $Ir(ppy)_3$ (30 nm)/Al (100 nm) was fabricated, where *x* was 8, 15, 20 and 25 wt.% $Ir(ppy)_3$. Fig. 3 shows the current density–voltage characteristics of these hole-only devices. As the doping concentration of $Ir(ppy)_3$ increased from 8 to 25 wt%, the corresponding devices A1 to A4 showed, in turn, increased current densities under the same voltage. When the voltage was >3.7 V, the device with 25 wt% $Ir(ppy)_3$ showed the highest hole current among the hole-only devices under the same voltage. This proves that the free holes were augmented as the doping concentration of $Ir(ppy)_3$ increased from 8 to 25 wt%. For the series A devices, there was a bigger hole injection barrier (1.1 eV) at the ITO/[CBP:$Ir(ppy)_3$] interface as a result of the absence of an HTL, leading to a large number of electrons gathering in the LEL. To balance the electron and hole carriers in the LEL, more holes need to be injected into the LEL. Fortunately, with the increased concentration of $Ir(ppy)_3$ doped into CBP, $Ir(ppy)_3$ as a trapping center effectively captures the electrons in the LEL, inducing the formation of a large number of free holes, which is helpful in balancing the electron and hole carriers in the LEL to give a high possibility of electron–hole recombination. The luminance and current efficiency of the series A4 devices were therefore significantly improved, which is mainly based on the direct charge-trapping effect of the $Ir(ppy)_3$ center and the improvement in the hole-transporting ability of the CBP:$Ir(ppy)_3$ layer.

3.2. Optimizing the thickness of MoO_3

It has previously been shown[19] that using MoO_3 as buffer layer for the ITO anode can effectively enhance hole injection. An MoO_3 layer of the appropriate thickness can decrease the hole injection barrier from the ITO to the LEL because the work-function of the ITO/MoO_3 interface can be increased to 6.8 eV as a result of the presence of a large surface dipole.[20] Series B devices with different thicknesses of MoO_3 layer were therefore also constructed: ITO MoO_3 (*y* nm)/CBP: 20 wt% $Ir(ppy)_3$ (30 nm)/TAZ (50 nm)/LiF (1 nm)/Al (100 nm), where *y* was 1, 3, 6 or 8 nm. Fig. 4 shows the luminance–voltage curves and current efficiency–current density curves of the series B devices and Table 1 summarizes their EL performances. It can be seen that the device with a 3 nm MoO_3 layer has a maximum luminance of 26 067 cd m^{-2} and a peak current efficiency of 39.2 cd A^{-1}, which is the highest performance of all the series B devices. The optimum thickness of the MoO_3 layer was therefore 3 nm.

3.3. Investigation of charge-accumulation effects

In agreement with the reported experiments, it should be noted that, as a result of the higher energy barrier (about 0.7 eV) of hole injection from $Ir(ppy)_3$ into CBP after the direct formation of excitons on the $Ir(ppy)_3$ center, some of the holes may be aggregated onto the $Ir(ppy)_3$ emitter rather than transferring to CBP. These accumulated holes in the HOMO

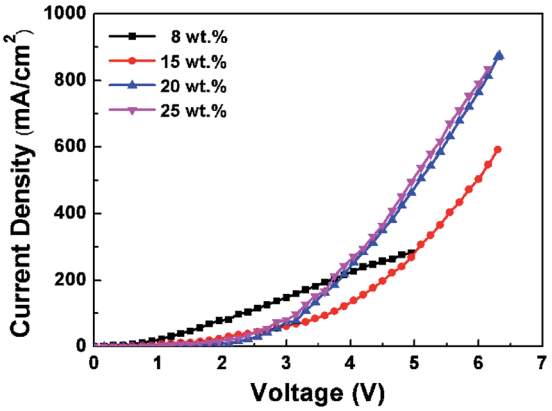

Fig. 3 Current–voltage curves of the hole-only devices with the structure ITO/MoO_3 (3 nm)/CBP: x wt% Ir(ppy)$_3$ (30 nm)/Al (100 nm) (x = 8, 15, 20 and 25 wt%).

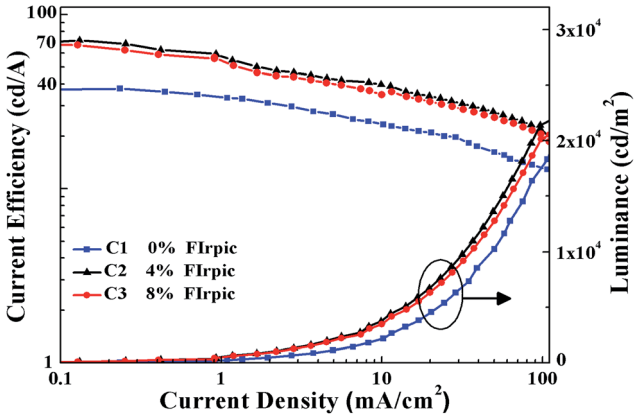

Fig. 5 Current efficiency–current density–luminance characteristics of series C devices.

level of Ir(ppy)$_3$ may quench the triplet excitons, which will lower the device performance.[21] To investigate this charge-accumulation effect, we fabricated series C devices with the structure ITO/MoO_3 (3 nm)/CBP: 20 wt% Ir(ppy)$_3$: z wt% FIrpic (30 nm)/TAZ (50 nm)/LiF (1 nm)/Al (100 nm), where z was 0, 4 and 8 wt%. In the series C devices, because the HOMO level of FIrpic (5.8 eV) was located between those of Ir(ppy)$_3$ (5.4 eV) and CBP (6.1 eV), the accumulated holes in Ir(ppy)$_3$ were efficiently transferred to CBP *via* FIrpic, which reduced the hole–exciton quenching. In addition, because the triplet energy level was higher for FIrpic (2.65 eV) than for Ir(ppy)$_3$ (2.4 eV),[22] the triplet excitons based on FIrpic could be transferred to Ir(ppy)$_3$ by a Dexter energy transfer mechanism, leading to a higher EL efficiency. Fig. 5 shows the current efficiency–current density–luminance characteristics of the series C devices; the EL performance is summarized in Table 1. As expected, when we incorporated 4 and 8 wt% FIrpic into the CBP: 25 wt% Ir(ppy)$_3$ layer for devices C2 and C3, respectively, devices C2 and C3 showed a remarkably improved current efficiency compared with device C1. The maximum current efficiency reached 71.2 cd A^{-1} for C2 and 66.9 cd A^{-1} for C3, corresponding with luminance increases to 27 524 and 25 905 cd m^{-2}, respectively.

To our knowledge, the efficiency achieved is greater than that of previously reported simplified OLEDs. We believe that the introduction of FIrpic is beneficial in eliminating the hole accumulation on Ir(ppy)$_3$ emitters. In addition, the EL spectra of series C devices (Fig. 6) show a single EL peak at 516 nm originating from Ir(ppy)$_3$, indicating an efficient Dexter energy transfer from FIrpic to Ir(ppy)$_3$. However, the maximum current efficiency and luminance of device C3 are

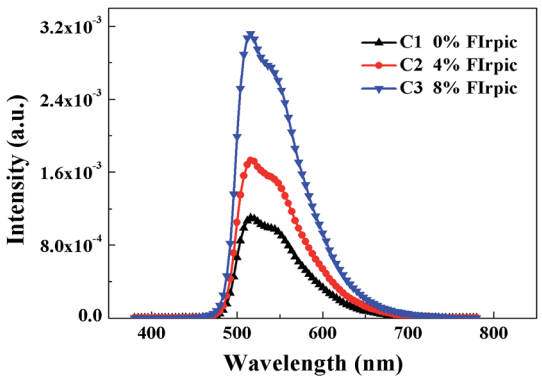

Fig. 6 EL spectra of series C devices under a 4 V bias.

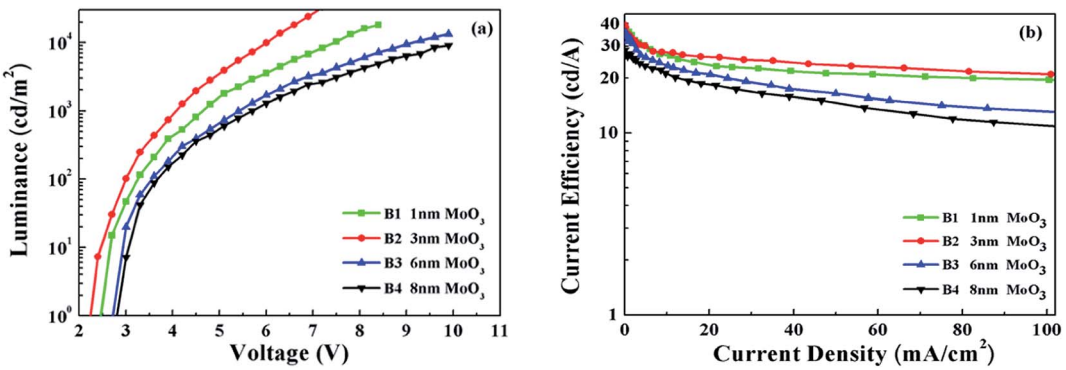

Fig. 4 (a) Luminance–voltage curves and (b) current efficiency–current density curves of series B devices.

lower than those of device C2, which might be attributed to an energy loss in the energy transfer process from $Ir(ppy)_3$ to CPB, CBP to FIrpic and FIrpic to $Ir(ppy)_3$ as a result of the higher doping concentration of FIrpic in device C3.

4. Conclusion

Simplified OLEDs based on heavy doping of $Ir(ppy)_3$ with the structure ITO/MoO_3 (3 nm)/CBP: 25% $Ir(ppy)_3$ (30 nm)/TAZ (50 nm)/LiF (1 nm)/Al (100 nm) have a low turn-on voltage of 2.4 V and a high current efficiency of 46.8 cd A^{-1} when FIrpic is incorporated into the CBP: 25 wt% $Ir(ppy)_3$ layer. The device shows a high efficiency of 71.2 cd A^{-1}, which is superior to previously reported simplified OLEDs. The improvement in performance can be attributed to the following two reasons: (1) the multi-functional properties of heavy doping with $Ir(ppy)_3$, which behaves as an emitter, has charge-trapping effects and assists with hole-transportation; and (2) the incorporation of FIrpic into CBP: 25 wt% $Ir(ppy)_3$, which relieves the effect of the aggregation of holes. The device with a heavy doping of phosphor still shows a higher EL performance, which is important for our further understanding of the physical mechanism of EL in PhOLEDs and is also significant in industrial production as a result of the simplified device structure.

Acknowledgements

This work was financially supported by the Program for Changjiang Scholar and Innovation Research Team in University (IRT0972), the International Science & Technology Cooperation Program of China (2012DFR50460), the Program for New Century Excellent Talents in University of Ministry of Education of China (NCET-13-0927), the National Natural Scientific Foundation of China (21101111, 61205179, 61307030, 61307029) and the Shanxi Provincial Key Innovative Research Team in Science and Technology (2012041011).

References

1 M. A. Baldo, S. Lamansky, P. E. Burrows, M. E. Thompson and S. R. Forrest, *Appl. Phys. Lett.*, 1999, **75**, 4.
2 C. Adachi, M. A. Baldo, M. E. Thompson and S. R. Forrest, *J. Appl. Phys.*, 2001, **90**, 5048.
3 M. A. Baldo, D. F. O'Brien, Y. You, A. Shoustikov, S. Sibley, M. E. Thompson and S. R. Forrest, *Nature*, 1998, **395**, 151.
4 C. Sahin, I. Onerb and C. Varlikli, *RSC Adv.*, 2014, **4**, 46831.
5 M. Ikai, S. Tokito, Y. Sakamoto, T. Suzuki and Y. Taga, *Appl. Phys. Lett.*, 2001, **79**, 156.
6 D. Tanaka, H. Sasabe, Y. J. Li, S. J. Su, T. Takade and J. Kido, *Jpn. J. Appl. Phys., Part 1*, 2007, **46**, 10.
7 C. H. Gao, D. Y. Zhou, W. Gu, X. B. Shi, Z. K. Wang and L. S. Liao, *Org. Electron.*, 2013, **14**, 1177.
8 R. Acharya and X. A. Cao, *Appl. Phys. Lett.*, 2012, **101**, 05330.
9 J. Meyer, S. Hamwi, T. Bülow, H. H. Johannes, T. Riedl and W. Kowalsky, *Appl. Phys. Lett.*, 2007, **91**, 113506.
10 Z. W. Liu, M. G. Helander, Z. B. Wang and Z. H. Lu, *Appl. Phys. Lett.*, 2009, **94**, 113305.
11 M. C. Suh, H. Y. Shin and S. J. Cha, *Org. Electron.*, 2013, **14**, 2198.
12 C. Adachi, M. A. Baldo, S. R. Forrest and M. E. Thompson, *Appl. Phys. Lett.*, 2000, **77**, 904.
13 E. Orselli, G. S. Kottas, A. E. Konradsson, P. Coppo, R. Frohlich, L. D. Cola, A. V. Dijken, M. Büchel and H. Borner, *Inorg. Chem.*, 2007, **46**, 11082.
14 Y. F. Lv, P. C. Zhou, N. Wei, K. J. Peng, J. N. Yu, B. Wei, Z. X. Wang and Ch. Li, *Org. Electron.*, 2013, **14**, 124.
15 M. C. Ikai, S. Z. Tokito, Y. C. Sakamoto, T. S. Suzuki and Y. S. Taga, *Appl. Phys. Lett.*, 2001, **79**, 156.
16 M. A. Baldo, C. Adachi and S. R. Forrest, *Phys. Rev. B: Condens. Matter Mater. Phys.*, 2000, **62**, 10967.
17 S. Reineke, K. Walzer and K. Leo, *Phys. Rev. B: Condens. Matter Mater. Phys.*, 2007, **75**, 5328.
18 J. H. Lee, J. I. Lee, K. I. Song, S. J. Lee and H. Y. Chu, *Appl. Phys. Lett.*, 2008, **92**, 133304.
19 T. Matsushima, G. Jin and H. Murata, *J. Appl. Phys.*, 2008, **104**, 054501.
20 I. Fan, M. L. Zhang, H. J. Ding, C. W. Tang and Y. L. Gao, *Org. Electron.*, 2001, **12**, 1588.
21 D. Y. Kondakov, J. R. Sandifer, C. W. Tang and R. H. Young, *J. Appl. Phys.*, 2003, **93**, 1108.
22 Q. Wang, J. Q. Ding, D. G. Ma, Y. X. Cheng and L. X. Wang, *Appl. Phys. Lett.*, 2009, **94**, 103503.